Efficient photo catalysts based on silver doped ZnO nanorods for the photo degradation of methyl orange

Muhammad Ali Bhatti, Aqeel Ahmed Shah, Khalida Faryal Almani, Aneela Tahira, Seyed Ebrahim Chalangar, Ali Dad Chandio, Omer Nur, Magnus Willander and Zafar Hussain Ibupoto

Bhatti, M. A., Shah, A. A., Almani, K. F., Tahira, A., Chalangar, S. E., Chandio, A. D., Nur, O., Willander, M., Ibupoto, Z. H., (2019), Efficient photo catalysts based on silver doped ZnO nanorods for the photo degradation of methyl orange, *Ceramics International*, 45(17), 23289-23297.
https://doi.org/10.1016/j.ceramint.2019.08.027

Efficient photo catalysts based on silver doped ZnO nanorods for the photo degradation of methyl orange

Muhammad Ali Bhatti[a], Aqeel Ahmed Shah[c], Khalida Faryal Almani[a], Aneela Tahira[d], Seyed Ebrahim Chalangar[d], Ali dad Chandio[c], Omer Nur[d], Magnus Willander[d], Zafar Hussain Ibupoto*[b]

[a]Department of Environmental Sciences University of Sindh Jamshoro, 76080, Sindh Pakistan

[b] Dr. M.A Kazi Institute of Chemistry University of Sindh Jamshoro, 76080, Sindh Pakistan

[c]NED University of Engineering and Technology Karachi, Pakistan

[d]Department of Science and Technology, Campus Norrkoping, Linkoping University, SE-60174 Norrkoping, Sweden

*Corresponding author: Zafar Hussain Ibupoto

Email address: zafar.ibhupoto@usindh.edu.pk

Abstract:

In this study, the doped ZnO nanorods with silver (Ag) as photosensitive material are prepared by the solvothermal method. The structural and optical characterization is carried out by the scanning electron microscopy, X-ray diffraction, energy dispersive spectroscopy and UV-visible spectroscopy. The use of Ag as dopant did not alter the morphology of ZnO except sample 4 which has flower like morphology. The Ag, Zn and O are the main constituent of doped materials. The XRD revealed a hexagonal phase for ZnO and cubic phase for silver and confirmed the successful doping of Ag. The photocatalytic activity of Ag doped ZnO nanorods was investigated for the photo degradation of methyl orange. The photocatalytic measurements show that 88% degradation of methyl orange by the sample 4 within the 2 h of UV light treatment (365nm) is significant advancement in the photocatalyst and provide the inexpensive and promising materials for the photochemical applications.

Keywords. ZnO nanorods, silver doping, methyl orange, photo degradation

1. Introduction

The scientific and technological development has produced high concerns to the environment pollution especially water pollution. The large number of pollutants are coming to our environment through untreated water from various industrial sources such as textile, photography, printing, painting, leather, agro allied companies – pesticides, insecticides and fertilizers. These pollutants go into our environment and becomes hazardous to people, animals, microorganisms and aquatic life [1-3]. Among these pollutants, the organic dyes are the compounds which gives color to water and to fibers. Several textile and fabric industries are established around the globe and they use approximately 30% dyes which is equivalent to 1000 tons per year [4,5]. Moreover, the textile industry through dyes gives 17%-20% industrial water pollution as reported by the World bank [6,7]. The most dyes contain the azoic dyes including methyl orange which carry nitrogen π-bond in the structure [8, 9]. The methyl orange (MO) is among the important azo dyes and extensively applied in the textile, food, leather and pharmaceutical companies. MO is also used as coloring agent for the determination of hydrogen gas and hydrochlorides [10, 11]. It is of great concern that MO is added into the water that causes huge impact on the quality of water and creates alarm situations for the aquatic life [12]. The worst aspects of using MO are its toxicity, mutagenic and carcinogenic nature [13–15]. The MO is hard to degrade; therefore, selective methods are needed for its degradation. The conventional methods are frequently used such as coagulation, reverse osmosis, membrane filtration, oxidation, reduction, complexometric, ion exchange, anaerobic, and aerobic [16] for the degradation of MO. Among these methods, photocatalytic degradation seems to be the promising technology for the degradation of water materials, and organic compounds specifically as it uses the natural sun light or artificial illumination including ultraviolet and microwave etc [17–19]. But the photocatalytic degradation requires a potential photosensitive material to degrade the pollutants in the presence of light. The extensive attempts are made to produce these materials for the photocatalytic degradation especially semiconducting nanostructures including TiO_2, SiO_2, ZnO, Fe_2O_3, CdS, ZnS, etc. [20–22]. Among these nanostructured materials, zinc oxide (ZnO) have received a great attention due to its unique properties and applications. ZnO is used in various potential applications such as light emitting diodes, photodetectors, chemical and biosensors, solar cells, piezoelectric nanogenerators, and actuators. Moreover, ZnO has been used extensively in several photochemical applications [23-26]. ZnO is wide bandgap materials with (3.37 eV), large binding energy (60 eV) at room

temperature, inexpensive, nontoxic and chemically resistive material [27-35]. Numerous studies are reported using ZnO for the photocatalytic degradation of MO in the presence of UV light [36-39]. Zhu et al. [40] reported ZnO rod- assembled microspheres and obtained them by microwave-assisted hydrothermal method and they took 9 h to degrade MO completely. Wand et al [41] prepared ZnO powder of different size through physical and chemical methods. The ZnO particle size has shown different photocatalytic degradation behavior and ZnO nanoparticles of 50 nm has 80% degraded MO in 2h. Hong et al. [42] synthesized Fe_3O_4/ZnO core shell nanocomposite via co-precipitation process and found 83% photo degradation of MO in 6 h. Fu et al. [43] synthesized Cu-doped ZnO nanoparticles and they revealed 88% degradation of MO in 4 h. Zheng et al. [44] fabricated ZnO nanorods on the indium tine oxide substrate by thermal evaporation and 71% degradation of MO was demonstrated in 2.5h. The doping of ZnO has shown promising features in photo degradation as it enhances the optical, electrical, and magnetic properties. The use of transition metal ions has great impact on the functional properties of ZnO as they are not used as trapping agents, but they minimize the charge recombination and accelerates the interfacial electron transfer which further increases the surface reactivity [45,46]. Also, doping has capability to absorb photons of light with extended solar spectrum. Several dopants have been used to improve the photocatalytic activity of ZnO such as Co [47], Ag [48], Mn [49], Pd [50], Bi [51], Sm [52], Al [53], Ce [54], and Ag [55]. These enough works on ZnO for the degradation application are carried out but, in our case, we used silver as dopant based on its plasmonic effect which consumes the large portion of light and there by efficient degradation is demonstrated. The plasmonic effect of silver for the degradation is rarely investigated and it will excite the scientific community to investigate more photo catalytic properties of ZnO using plasmonic effect, thus present work is quite different from the reported works based on ZnO. Also, the optimization approach is used to illustrate the effect of dopant on the plasmonic effect which indicates a fast photo degradation kinetics by tailoring the dopant concentration into the ZnO. The method for the silver doping into ZnO is solvothermal method which is different from the reported works.

In this study, we report the Ag doped ZnO nanostructures by low temperature aqueous chemical growth method. The silver is successfully incorporated in the structure of ZnO and it has shown significant photocatalytic degradation of MO. Sample 4 has almost 88% photo degradation efficiency. This indicates that by optimizing the dopant level in ZnO can lead to the development

of photosensitive materials. The synthetic strategy is simple and cost effective and it can pave the way for the widespread use of these Ag doped ZnO nanostructures in diverse applications.

2. Experimental section

Silver nitrate ($AgNO_3$, M=169.87, Merck), Zinc acetate-dihydrate ($ZnC_4H_6O_4$, M=183.48, Merck), ammonia solution (25%, Merck), methyl orange, and ethanol (C2H5OH, 99.5%, were purchased from Sigma-Aldrich). All the chemicals were used without further purification and throughout the study, the solutions were prepared in the deionized water.

2.1. Synthesis of Ag doped ZnO nanostructures

The Ag doped ZnO nanostructures were obtained by precipitation process. The zinc acetate di-hydrate and 25% ammonia were used as the primary reagents and the following strategy was used to produce Ag doped ZnO. The dispersion of different contents of silver namely 5, 10, 15 and 20 mg was carried out in 5 mL of ethanol and it was left for sonication for 30 mints. Then 2.22 g of zinc acetate di-hydrate were dissolved into 100 mL of the deionized water and 5 mL of 25 % ammonia was mixed with zinc precursor. Five beakers were containing the zinc acetate di-hydrate and ammonia. In four beakers 5, 10, 15 and 20 mg of silver nitrate were dispersed in 5 mL of ethanol and they were labelled as sample 1, 2, 3, and 4. One beaker containing zinc acetate di-hydrate and ammonia labelled as pristine sample. Then beakers were covered with the aluminum foil in order to avoid the evaporation of growth solution. The beakers were kept at 90 ^oC for 5 hours in preheated electric oven. After the growth, the beakers were taken out from the oven and white product was settled in the bottom of each beaker. Then filtration was used to collect the white nanomaterial product.

The crystal structure, morphology and composition of prepared Ag doped samples were studied by powder X-ray diffraction (XRD), scanning electron microscopy (SEM) and energy dispersive spectroscopy (EDS). The SEM images were collected at an accelerating voltage of 3 kV and EDS was equipped with SEM for the recording of EDS spectra.

2.2. Photo degradation activity of prepared ZnO nanostructures

The photo degradation of various ZnO samples was investigated for the degradation of aqueous MO. The photo degradation was carried out in the presence of UV lamps with wavelength of 365 nm and power of each lamp was 10 W. The 10 mg of photocatalyst was dispersed in MO solution and a uniform distribution was obtained, the solution was stirred in ultrasonic bath for 10 mints. The adsorption and desorption process on the photocatalyst surface were monitored by the

magnetic stirring for 30 mints in the dark. Then solution was treated with UV lamps at different intervals of time. After the UV light treatment, the suspensions were used by UV-visible spectrophotometer (PE Lamda35) by recording the absorption at characteristic wavelength of 470 nm to estimate the amount of the MO in suspension. The photo degradation efficiency of various Ag doped ZnO samples was measured by the following equation:

Degradation efficiency % $= \frac{Co-Ct}{Co} \times 100$

Here Co is the initial MO concentration (mg/L), *Ct* shows the MO concentration (mg/L) after different intervals of UV light treatment (t).

To further investigate the kinetics of photo degradation of MO and pseudo first order kinetics was measured using the following expression

$ln\_C0/Ct\_ = Kapp \times t$

Here *Kapp* indicates the reaction rate constant, *C0* is the initial concentration of MO(mg/L) at irradiation time 0 min, and *Ct* shows the MO concentration at the reaction time *t* (mg/L).

3. Result and discussion

The powder XRD was used to record the reflection peaks of various ZnO samples as depicted in Figure 1. The diffraction patterns of ZnO in Ag doped samples are same as that in undoped ZnO sample, however some metallic silver patterns are found which confirms the successful doping of Ag into ZnO nanostructures. The reflection peaks for Ag doped ZnO are measured at 2 thetas 31.737° (54.8), 34.420° (43.8), 36.225° (100), 47.515° (21.9), 56.536° (27,7), 62.836° (30.8), 66.304° (3.5), 67.893° (20.4), 69.015° (9.3), and 72.561° (2.2), 76.891°(3) as shown in Figure 1. The diffraction patterns of ZnO are in agreement with reference card no. 96-900-4182 and ZnO exhibits hexagonal phase. There is shift of diffraction angle, which is due to the difference in the size of Ag and Zn atoms that further creates the distance in crystal structure and might decrease in diffraction angl, here in our case Ag is bigger in size than Zn atom, therefore we see shift in the diffraction to small angle. The XRD has identified the diffraction patterns for the silver in the ZnO as described by blue color and they are well matched to the reference card no. 96-901-1609 and it has cubic phase.

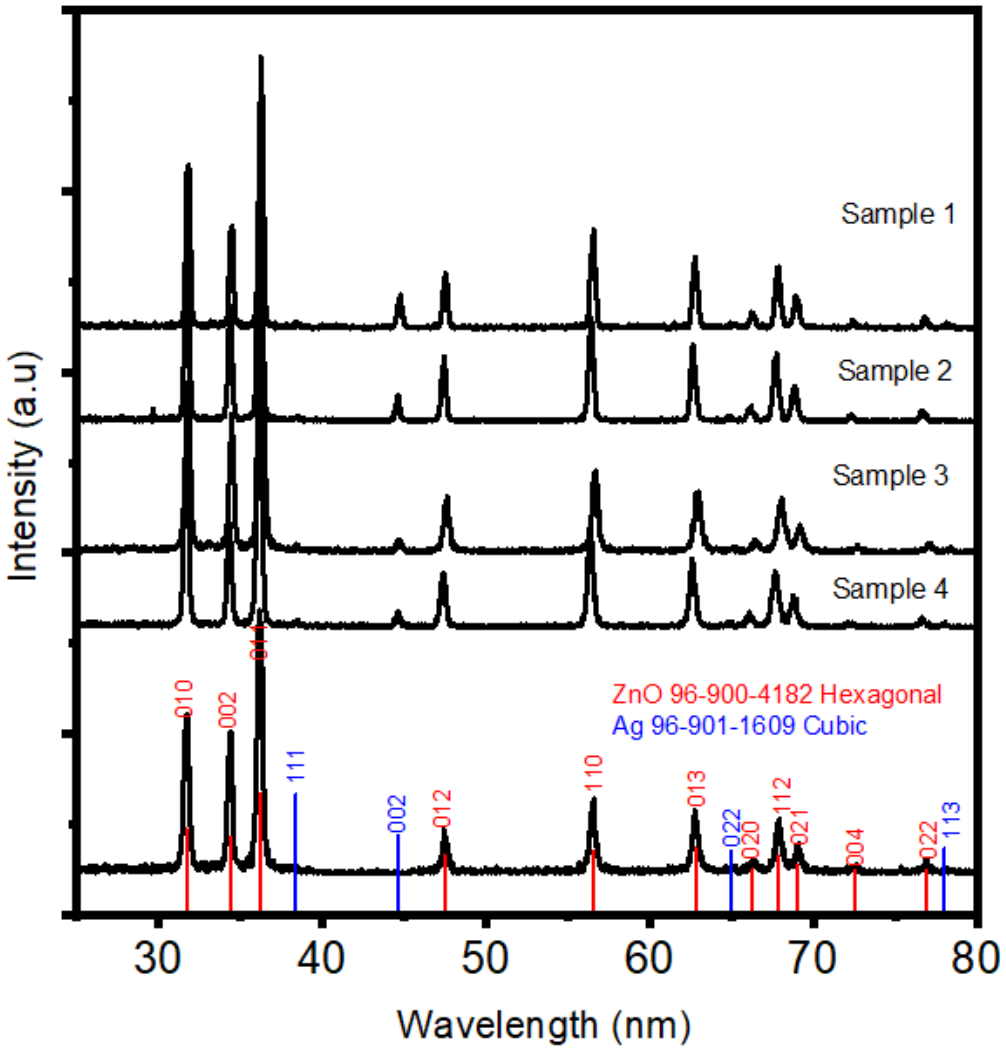

Figure.1 The XRD patterns of pure ZnO and Ag-doped ZnO nanostructures, sample-1-4.

The morphological features of different ZnO nanostructures were investigated by SEM as shown in Figure 2. Both the undoped and doped ZnO nanostructures are integrated into Figure 2. The morphology remains unaltered after the doping except sample 4 that has flower like morphology due to excess of silver nitrate concentration in ethanol. ZnO nanostructures exhibit nanorod like shape and the length of each nanorod is few microns and an average diameter is 100 to 200 nm. The composition of Ag doped ZnO samples was analyzed by EDS mapping which confirms the uniform distribution of Ag, Zn, and O in the nanorod morphology.

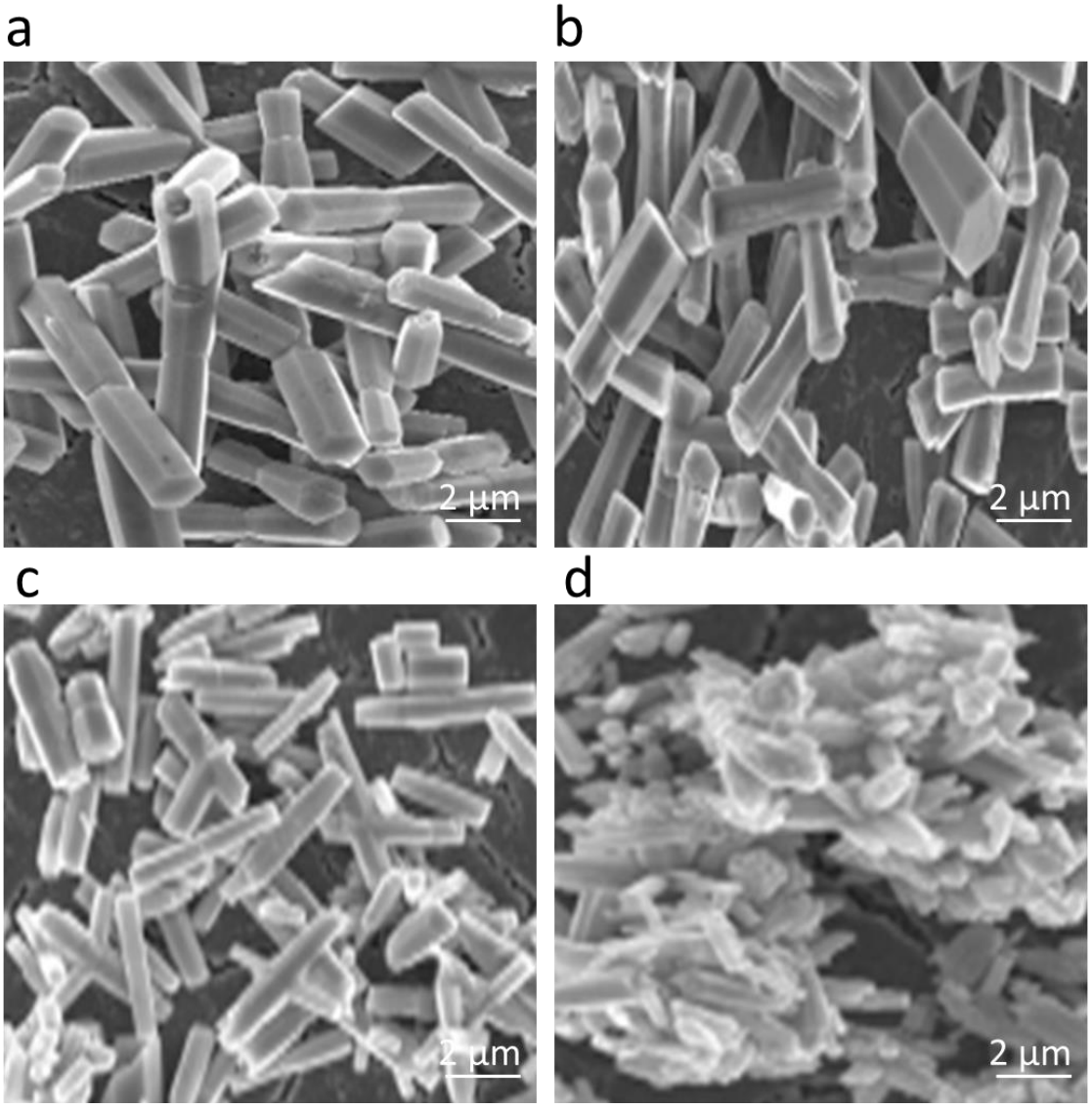

Figure 2: The SEM images of various Ag doped ZnO nanostructures (a) sample 1, (b) sample 2, (c) sample 3 and (d) sample 4

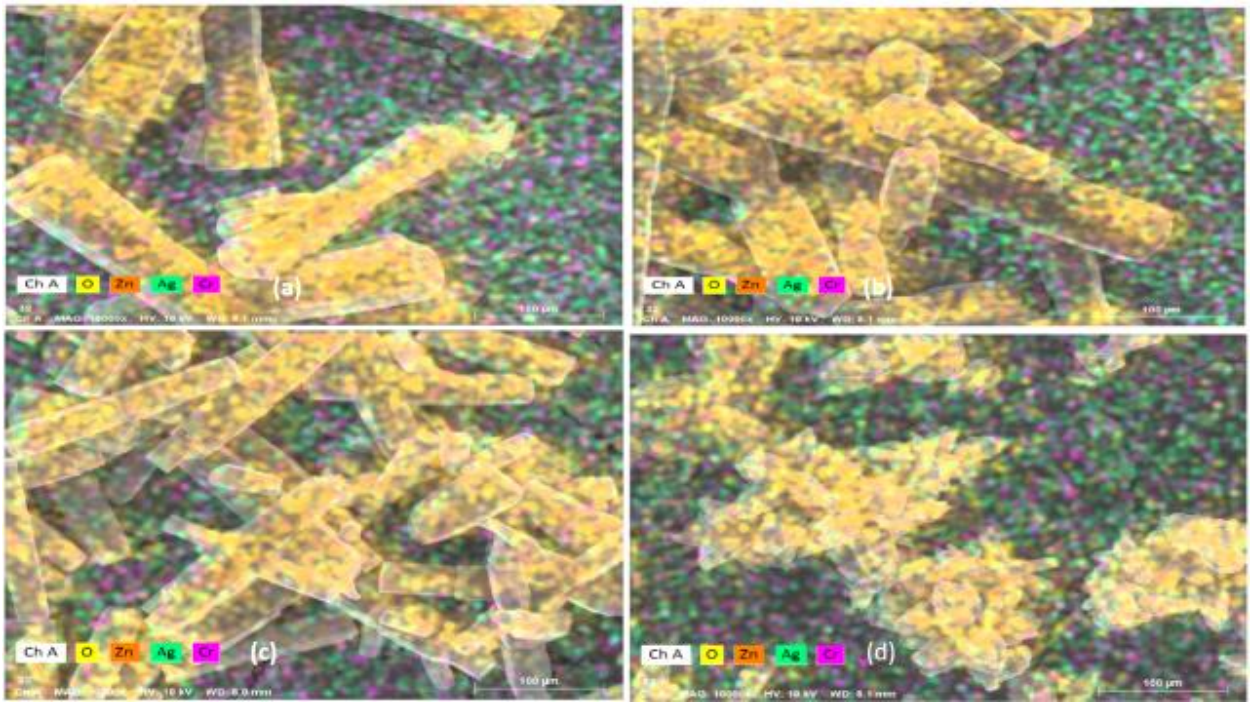

Figure 3: The elemental mapping of various Ag doped ZnO nanostructures (a) sample 1, (b) sample 2, (c) sample 3 and (d) sample 4

Further to understand the excellent photocatalytic activity of Ag doped ZnO via estimation of optical bandgap as the concentration of Ag is increased the band gap is decreased from 3.38 to 3.11 eV. The variation in bandgap with increase in the dopant level can be assigned to the addition of dopant into the ZnO lattice which further facilitates the electron from valence band to the conduction band as shown in Figure 4. The calculated values of optical band gap are shown in Table 1. To investigate the photosensitive response for the degradation for MO, an optimum approach was used to illustrate the role for different Ag dopant levels on the dye degradation and their performance was compared with the pristine ZnO (un doped ZnO) as shown in Figure 5. The pristine ZnO has shown poor degradation efficiency and slow degradation kinetics. Using 10 mg of pristine ZnO and 0.05 mM MO and the UV-visible absorption spectra were recorded, and maximum absorption was measured at 330-360 nm and only 61% degradation efficiency for the 6 h using UV light. This prolong degradation of pristine ZnO has shown space for the development of new functional materials for an excellent photo degradation efficiency and fast kinetics. Moreover, the poor performance of pristine ZnO for the degradation of methyl orange is attributed to the fast recombination rate of photogenerated electron and hole pairs and low quantum yield for the photocatalytic reaction in water media. Likewise, the UV-visible spectra for the various Ag

doped ZnO samples were measured for the degradation of MO in the presence of UV light. With time, the absorption was steeply decreasing which indicate that fast degradation of MO with Ag doped ZnO samples and in 2 h almost complete degradation is demonstrated by the sample 3 and 4 as shown in Figure 6. The degradation efficiency was found 88.08% and 85.26% for the samples 3 and 4 in 2 h as shown in Figure 6. The sample 1 and 2 have also significant effect on the degradation but the sample 3 and 4 has confirmed that increasing the Ag amount during the doping can lead to the excellent efficiency and rapid rate of degradation. However, when comparing the degradation of Ag doped samples with pristine ZnO for MO, the Ag is showing dominant role on the degradation efficiency and rate of degradation, thus doping into ZnO is promising strategy to design new photocatalysts for the environmental applications especially the degradation of water pollutants. Figure 6 shows the kinetic plot between ln (C/Co) vs and time that indicates the pseudo first order kinetics and extracting the slope which can be corresponded to the rate constant. The high value of rate constants indicates the favorable kinetics of photo degradation of MO using silver doped ZnO samples. The photo degradation efficiency was higher for the sample 3 and 4 as shown in Figure 6 and it reveals that Ag due to large plasmonic effect has shown significant impact on the photo degradation efficiency MO. The use of Ag doped ZnO nanostructures for the degradation of MO and the mechanism in which role of Ag for the degradation of MO can be sum up in the following steps. Different researches have different opinion about the ZnO material to investigate for the photocatalytic applications such as to create oxygen defects or to deposit the metal nanoparticles on ZnO which lead to the separation of photo generated electron-hole pairs and consequently rapid photocatalytic activity is expected [56, 57]. The photocatalytic mechanism for the Ag/ZnO samples is described by the following equations [55]:

$ZnO + hv \rightarrow e_{cb}^{-} + h_{vb}$ (1)

$V_o^{\cdot\cdot} + e_{cb}^{-} \rightarrow V_o$ (2)

$V_o^{\cdot} + O_2 \rightarrow V_o^{\cdot\cdot} + \cdot O_2$ (3)

$Ag \rightarrow Ag^{+} e^{-}$ (or e_{cb}^{-}) (4)

e^{-} (or c_{cb}^{-}) $+ O_2 \rightarrow \cdot O_2$ (5)

$e_{cb}^{-} + Ag^{+} \rightarrow Ag$ (6)

$h^{+}_{vb} + OH^{-} \rightarrow \cdot OH$ (7

Based on these equations, the process of photocatalytic activity can be summarized as (a ZnO is used as the electron and hole supplier during the photo degradation of MO. During the treatment of semiconducting ZnO materials with UV light of equal or higher energy to that of optical bandgap then electrons (e) from valence band are excited to the conducing band which at the same time generate holes (h) in the valence band, (b) the oxygen defects as shown in equation 2 and 3 as Vo, and Vo,, and the Ag atoms in the crystal of ZnO are used to sink the electrons as given in equation 4 and 6 which facilitates the electron-hole pairs as depicted in equation 1, (c)The photoelectron are trapped as electron accepting species such as adsorbed O_2 which further creates superoxide radical anon (.O2) as shown in equation 5. Moreover, the photo induced holes are trapped by hydroxyl ion which turned into hydroxyl radical as (. OH) as given in equation 7. These produced superoxide and hydroxyl radicals are governing on the overall efficiency of photocatalytic reactions. For example, the hydroxyl radical is known as strong oxidizing agent either partial or complete degradation of organic compounds is unavoidable [55]. More insight on the mechanism for the improved performance of the Ag doped ZnO nanorods in photo degradation of methyl orange could be explained as. The valence band electrons of Ag during the interaction with UV light have equal or greater energy than the ZnO band gap then consequently the electrons from the valence band of silver are excited to the conduction band gap of ZnO that result in the generation of equal number of holes in the valence band of ZnO nanorods at the same time. As the conduction band energy level of pristine ZnO nanorods is higher than that of intraband state of Ag-doped ZnO thereby electron can move from ZnO to Ag. Due to the presence of Ag on the surface of ZnO nanorods that leads to the trapping of electrons and further it prevents the recombination of electron and holes pairs. Also, the methyl orange molecules might be excited during the interaction of UV light and can give the electrons to the conduction band of the ZnO and intraband state of the Ag. Due to the smaller intraband of Ag an enhanced photo catalytic degradation efficiency and rate is obtained for the Ag doped ZnO nanorods figure 7 shows the kinetic study of the silver doped ZnO nanostructures and their photo degradation efficiency as it can be seen that doped photo catalysts follows the pseudo first order kinetics and maximum photo degradation efficiency is shown by the sample 3 and sample 4.

Table:1. Optical parameters of pure ZnO and Ag doped ZnO nanostructures for the calculation of optical bandgap

Name of Samples	Cut-off wavelength (nm)	Band gap (eV)
Pure-ZnO	358.9	3.45
Sample-1	367	3.38
Sample-2	390.8	3.25
Sample-3	392.8	3.15
Sample-4	397.8	3.11

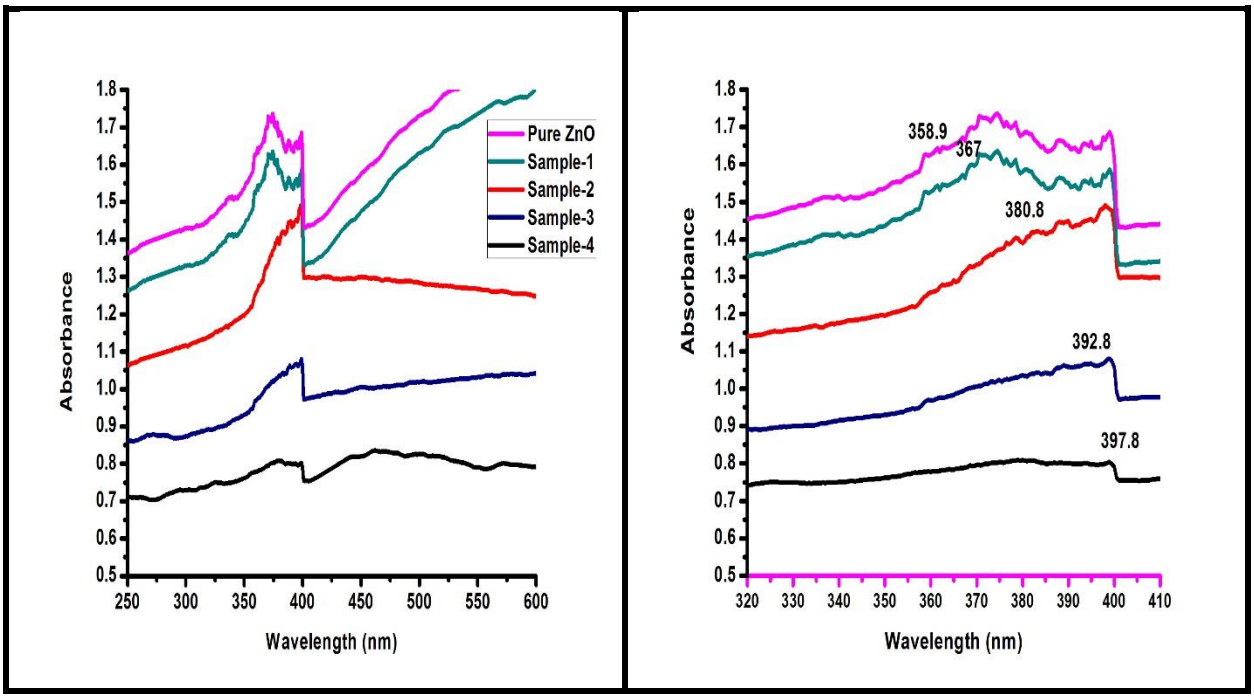

Figure 4: UV-visible absorption spectra for various Ag doped ZnO samples

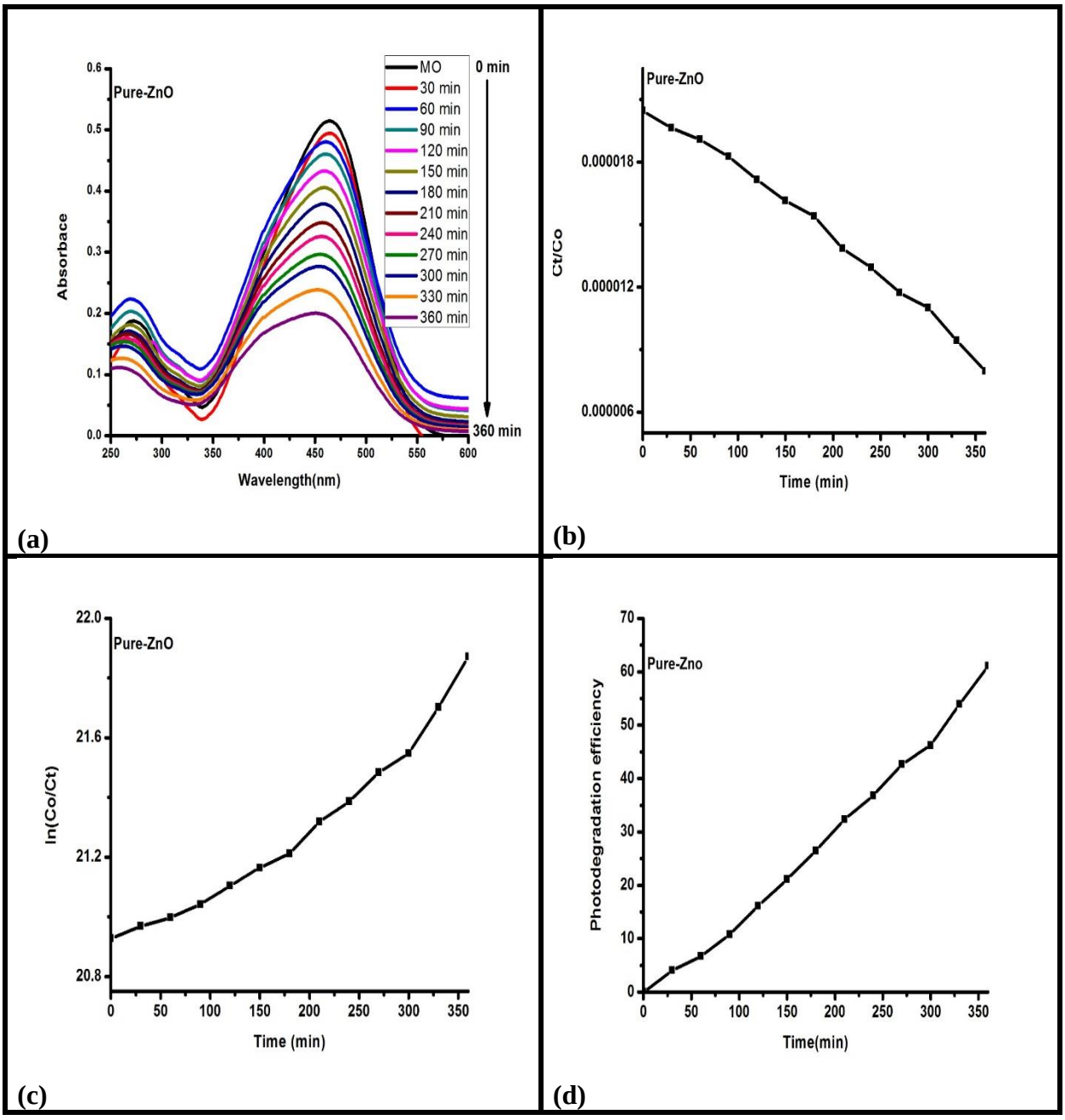

Figure 5: (a) shows the UV-visible absorption spectra of MO dye solution at different time after irradiating with UV light for the pristine ZnO, 5 (b) The $Ct/C0$ versus time curves of MO, 5(c) Kinetic plot of *Ln(Co/Ct)* versus irradiation time for photodegradation, 5(d) calibration curve of photo degradation efficiency (%) versus different intervals of time.

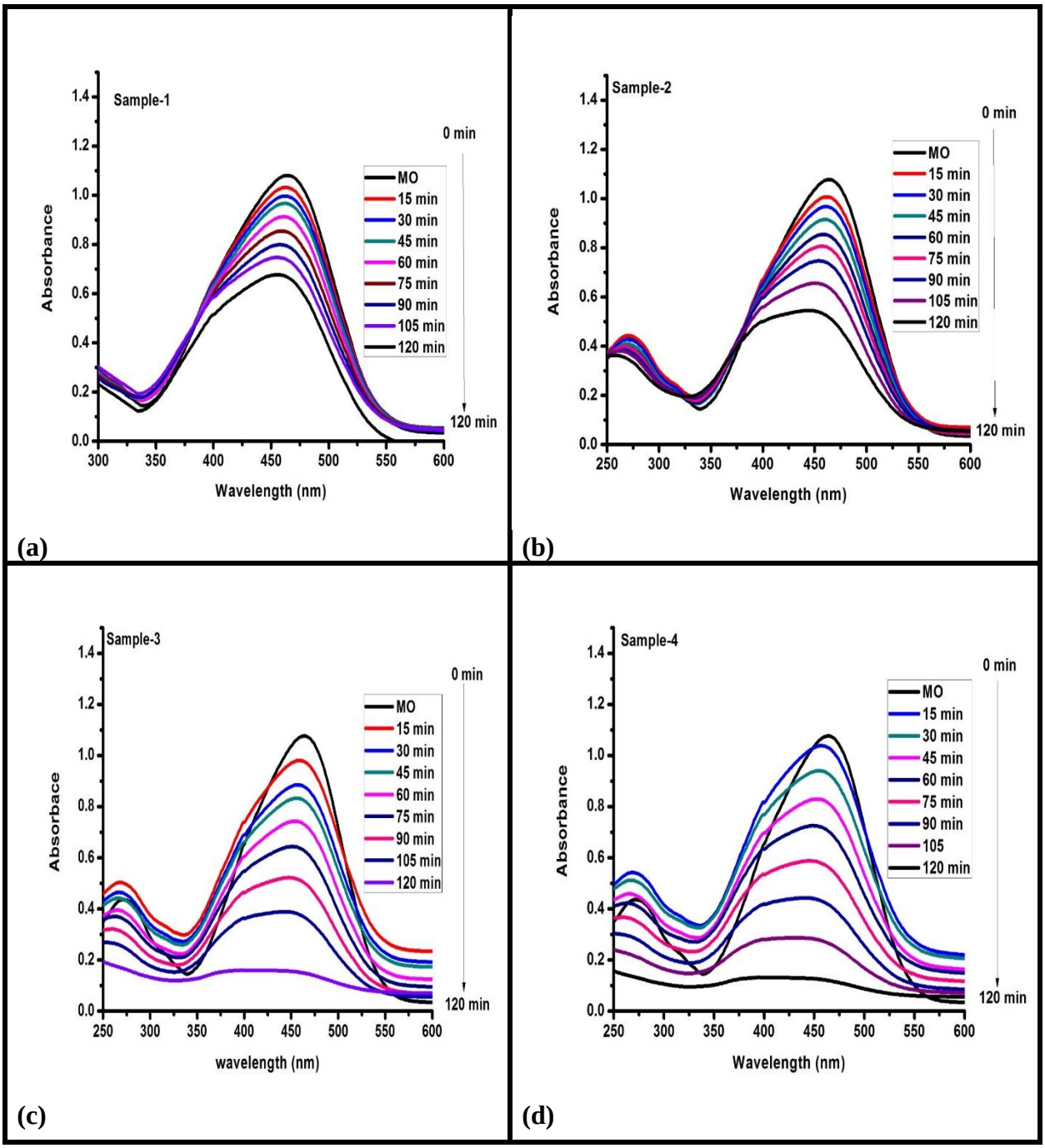

Figure: 6 (a, b, c, d) indicates the UV-visible absorbance spectra of MO dye solution at different intervals of time after irradiating with UV light and using various photocatalysts

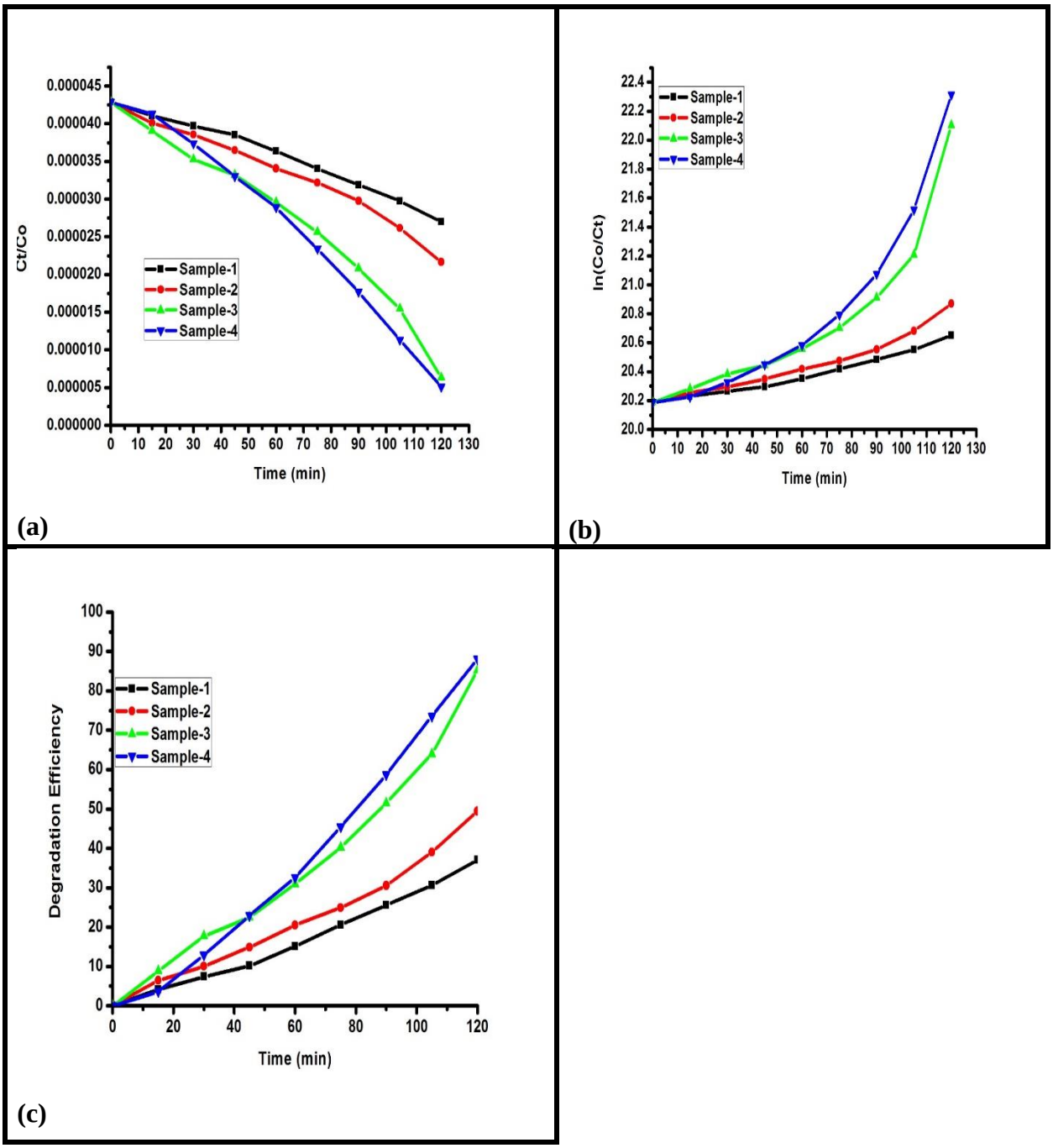

Figure: 7 (a) shows the $Ct/C0$ versus time curves of MO. (b) shows the Kinetic plot of *Ln(Co/Ct)* versus irradiation time and (c) shows the calibration curve of degradation rate (%) versus different intervals of time.

4. Conclusions

In summary, un doped and doped ZnO nanorods are prepared by the solvothermal method. XRD study has successfully confirmed the doping of silver and it does not alter the crystal structure of ZnO. Importantly, dopant did not show a significant effect on the morphology of ZnO nanorods except sample 4 which has flower like structure. EDS verified the composition of doped samples as shown by the XRD experiment. UV-visible spectroscopy analysis shows that the optical bandgap of ZnO decreases with the increase of dopant concentration. The pristine ZnO has poor photocatalytic activity when compared to the silver doped ZnO nanorods and almost 88% MO is degraded in the time 2 h. The doped ZnO nanorods are potential photocatalysts for the water purification and environmental applications.

5. References

[1]. Pascariu, A. Airinei, N. Olaru, L. Olaru, V. Nica, Photocatalytic degradation of rhodamine B dye using ZnO–SnO_2 electrospun ceramic nanofibers, *Ceram. Int.* 42 (2016) 6775–6781. https://doi.org/10.1016/j.ceramint.2016.01.054

[2]. Ahmed, M. A., Emad E. El-Katori, and Zarha H. Gharni. "Photocatalytic degradation of methylene blue dye using Fe_2O_3/TiO_2 nanoparticles prepared by sol–gel method." *Journal of Alloys and Compounds* 553 (2013): 19-29.https://doi.org/10.1016/j.jallcom.2012.10.038

[3]. Kazemi, M., and M. R. Mohammadizadeh. "Simultaneous improvement of photocatalytic and superhydrophilicity properties of nano TiO_2 thin films." *Chemical Engineering Research and Design* 90.10 (2012): 1473-1479. https://doi.org/10.1016/j.cherd.2012.02.002

[4]. A. Baban, A. Yediler, N.K. Ciliz, Integrated water management and CP implementation for wool and textile blend processes, *Clean* 38 (2010) 84–90. https://doi.org/10.1002/clen.200900102

[5]. T. Robinson, G. McMullan, R. Marchant, P. Nigam, Remediation of dyes in textile effluent: a critical review on current treatment technologies with a proposed alternative, *BioRes. Technol.* 77 (2011) 247–255. https://doi.org/10.1016/S0960-8524(00)00080-8

[6]. Chan, S.H.S.; Yeong Wu, T.; Juan, J.C.; Teh, C.Y. Recent developments of metal oxide semiconductors as photocatalysts in advanced oxidation processes (AOPs) for treatment of dye waste water. J. Chem. Technol. *Biotechnol*. 2011, 86, 1130–1158.

https://doi.org/10.1002/jctb.2636

[7]. Huang, S.T.; Lee, W.W.; Chang, J.L.; Huang, W.S.; Chou, S.Y.; Chen, C.C. Hydrothermal synthesis of $SrTiO_3$ nanocubes: Characterization, photocatalytic activities, and degradation pathway. *J. Taiwan Inst. Chem. Eng.* 2014, 45, 1927–1936. https://doi.org/10.1016/j.jtice.2014.02.003

[8]. Song, S., Xu, L., He, Z., Ying, H., Chen, J., Xiao, X., Yan, B., 2008. Photocatalytic degradation of C.I. Direct Red 23 in aqueous solutions under UV irradiation using $SrTiO_3/CeO_2$ composite as the catalyst. *J. Hazard. Mater*. 152, 1301-1308. https://doi.org/10.1016/j.jhazmat.2007.08.004

[9]. Lee, J.W., Choi, S.P., Thiruvenkatachari, R., Shim, WG., Moon, H., 2006. Eval-uation of the performance of adsorption and coagulation processes for the maximum removal of reactive dyes. *Dyes Pigm*. 69, 196–203. https://doi.org/10.1016/j.dyepig.2005.03.008

[10]. T. Katsuda, H. Ooshima, M. Azuma, J. Kato, New detection method for hydrogen gas for screening hydrogen-producing microorganisms using water-soluble wilkinson's catalyst derivative." *Journal of bioscience and bioengineering* 102.3 (2006): 220-226. https://doi.org/10.1263/jbb.102.220

[11]. B. Choudhary, A. Goyal, S.L. Khokra, "New visible spectrophotometric method for estimation of itopride hydrochloride from tablets formulations using methyl orange reagent." *International Journal of Pharmacy and Pharmaceutical Sciences* 1 (2009): 159-162.

[12]. Konstantinou IK, Albanis TA (2004) TiO_2-assisted photocatalytic degradation of azo dyes in aqueous solution: kinetic and mechanistic investigations: a re-view. Appl Catal B Environ 49(1):1–14. https://doi.org/10.1016/j.apcatb.2003.11.010

[13]. Biswas P, Wu C-Y. "Nanoparticles and the environment." *Journal of the Air & Waste Management Association* 55.6 (2005): 708-746. https://doi.org/10.1080/10473289.2005.10464656

[14]. Ahmad A, Mohd-Setapar SH, Chuong CS, Khatoon A, Wani WA, Kumar R, Rafatullah M. "Recent advances in new generation dye removal technologies: novel search for approaches to reprocess wastewater." *RSC Advances* 5.39 (2015): 30801-30818. https://doi.org/10.1039/C4RA16959J

[15]. Y.M. Slokar, A.M.L. Marechal. "Methods of decoloration of textile wastewaters." *Dyes and pigments* 37.4 (1998): 335-356. https://doi.org/10.1016/S0143-7208(97)00075-2

[16]. Riaz, U.; Ashraf, S.; Aqib, M. Microwave-assisted degradation of acid orange using a conjugated polymer, polyaniline, as catalyst. Arab. *J. Chem.* 2014, 7, 79–86. https://doi.org/10.1016/j.arabjc.2013.07.001

[17]. Shahabuddin, S.; Sarih, N.M.; Ismail, F.H.; Shahid, M.M.; Huang, N.M. Synthesis of chitosan grafted polyaniline/Co_3O_4 nanocube nanocomposites and their photocatalytic activity toward methylene blue dye degradation. *RSC Adv.* 2015, 5, 83857–83867. https://doi.org/10.1039/C5RA11237K

[18]. Zhou, M.; Han, D.; Liu, X.; Ma, C.; Wang, H.; Tang, Y.; Huo, P.; Shi, W.; Yan, Y.; Yang, J. Enhanced visible light photocatalytic activity of alkaline earth metal ions-doped CdSe/RGO photocatalysts synthesized by hydrothermal method. *Appl. Catal. B* 2015, 172, 174–184. https://doi.org/10.1016/j.apcatb.2015.01.004

[19]. Gardin S, Signorini R, Pistore A, Giustina GD, Brusatin G, Guglielmi M, Bozio R, "Photocatalytic Performance of Hybrid SiO_2− TiO_2 Films." *The Journal of Physical Chemistry C*114.17 (2010): 7646-7652. DOI: 10.1021/jp911495h

[20]. Pal S, Laera AM, Licciulli A, Catalano M, Taurino A. "Biphase TiO2 microspheres with enhanced photocatalytic activity." *Industrial & Engineering Chemistry Research* 53.19 (2014): 7931-7938. DOI: 10.1021/ie404123f

[21]. Kumar A, Mohanty T. "Electro-optic modulation induced enhancement in photocatalytic activity of N-doped TiO_2 thin films." *The Journal of Physical Chemistry C* 118.13 (2014): 7130-7138. DOI: 10.1021/jp4103977

[22]. Pei Z, Ding L, Lu M, FanZ,Weng S, Hu J, Liu P, "Synergistic effect in polyaniline-hybrid defective ZnO with enhanced photocatalytic activity and stability." *The Journal of Physical Chemistry C* 118.18 (2014): 9570-9577. DOI: 10.1021/jp5020143

[23] Zhigang Z, "Efficiency enhancement of ZnO/Cu_2O solar cells with well oriented and micrometer grain sized Cu_2O films". Appl. Phys. Lett. 112, (2018) 042106. https://doi.org/10.1063/1.5017002

[24]. Cunlong L, Ceng H, Yubo Z, Zhigang Z, Ming W, Xiaosheng T, Jihe D, "Enhanced photo response of self-powered perovskite photodetector based on ZnO nanoparticles decorated CsPbBr3films". *Solar Energy Materials and Solar Cells*, 172, (2017), 341-346. https://doi.org/10.1016/j.solmat.2017.08.014

[25]. Zhigang Z, Xiaosheng T, "Enhanced fluorescence imaging performance of hydrophobic colloidal ZnO nanoparticles by a facile method". *Journal of Alloys and Compounds,* 619, (2015), 98-101. https://doi.org/10.1016/j.jallcom.2014.09.072

[26]. Zhigang Z, Mengqing W, Weiwei C,Yangfu Z, Zhiqiang Z, Xiaofeng Z, Xiaosheng T, "Strong yellow emission of ZnO hollow nanospheres fabricated using polystyrene spheres as templates". *Materials & Design*, 84, (2015), 418-421. https://doi.org/10.1016/j.matdes.2015.06.141.

[27]. Ahmad R, Tripathy N, Jung DUJ, Hahn YB. "Highly sensitive hydrazine chemical sensor based on ZnO nanorods field-effect transistor." *Chemical Communications*50.15 (2014): 1890-1893. https://doi.org/10.1039/C3CC48197B

[28]. Hua G, Zhang Y, Zhang J, Cao X, XuW, Zhang L. "Fabrication of ZnO nanowire arrays by cycle growth in surfactantless aqueous solution and their applications on dye-sensitized solar cells." *Materials Letters*62.25 (2008): 4109-4111. https://doi.org/10.1016/j.matlet.2008.06.018

[29]. Chen L, Zhang C, DuZ, LiH, Zou W. Mater Lett2013;110:208–11.

[30]. Ahmad R, Tripathy N, HahnYB. "High-performance cholesterol sensor based on the solution-gated field effect transistor fabricated with ZnO nanorods." *Biosensors and Bioelectronics* 45 (2013): 281-286.https://doi.org/10.1016/j.bios.2013.01.021

[31]. Han HV, Hoa ND, Tong PV, Nguyen H, Hieu NV. Single-crystal zinc oxide nanorods with nanovoids as highly sensitive NO_2 nanosensors. Mater Lett. 2013;94:41-43. https://doi.org/10.1016/j.matlet.2012.12.006

[32]. Hahn YB, Ahmad R, Tripathy N. "Chemical and biological sensors based on metal oxide nanostructures." *Chemical Communications* 48.84 (2012): 10369-10385. https://doi.org/10.1039/C2CC34706G

[33]. N. Hassan, M. Hashim, Y. Al-Douri, Morphology and optical investigations of ZnO pyramids and nanoflakes for optoelectronic applications, *Opt.: Int. J. Light Electron Opt.* 125 (11) (2014) 2560–2564. https://doi.org/10.1016/j.ijleo.2013.10.023

[34]. F. Jiménez-García, et al., Influence of substrate on structural, morphological and optical properties of ZnO films grown by SILAR method, Bull. *Mater. Sci*. 37 (6) (2014) 12831291. https://doi.org/10.1007/s1203

[35]. S. Xu, Z.L. Wang, One-dimensional ZnO nanostructures: solution growth and functional properties, *Nano Res*. 4 (11) (2011) 1013–1098. https://doi.org/10.1007/s12274-011-0160-7

[36]. H.J. Wang, Y.Y. Sun, Y. Cao, X.H. Yu, X.M. Ji, L. Yang, "Porous zinc oxide films: Controlled synthesis, cytotoxicity and photocatalytic activity." *Chemical engineering journal* 178 (2011): 8-14. https://doi.org/10.1016/j.cej.2011.09.088

[37]. J. Lv, W. Gong, K. Huang, J. Zhu, F. Meng, X. Song, Z. Sun, "Effect of annealing temperature on photocatalytic activity of ZnO thin films prepared by sol–gel method." *Superlattices and Microstructures* 50.2 (2011): 98-106. https://doi.org/10.1016/j.spmi.2011.05.003

[38]. J. Xie, H. Wang, M. Duan, L. Zhang, "Synthesis and photocatalysis properties of ZnO structures with different morphologies via hydrothermal method." *Applied surface science* 257.15 (2011): 6358-6363. https://doi.org/10.1016/j.apsusc.2011.01.105

[39]. T. Sun, J. Qiu, C. Liang, "Controllable fabrication and photocatalytic activity of ZnO nanobelt arrays." *The Journal of Physical Chemistry C* 112.3 (2008): 715-721. DOI: 10.1021/jp710071f

[40]. Z. Zhu, D. Yang, H. Liu, "Microwave-assisted hydrothermal synthesis of ZnO rod-assembled microspheres and their photocatalytic performances." *Advanced Powder Technology* 22.4 (2011): 493-497. https://doi.org/10.1016/j.apt.2010.07.002

[41]. H. Wang, C. Xie, W. Zhang, S. Cai, Z. Yang, Y. Gui, "Comparison of dye degradation efficiency using ZnO powders with various size scales." *Journal of Hazardous materials* 141.3 (2007): 645-652. https://doi.org/10.1016/j.jhazmat.2006.07.021

[42]. R.Y. Hong, S.Z. Zhang, G.Q. Di, H.Z. Li, Y. Zheng, J. Ding, D.G. "Preparation, characterization and application of Fe_3O_4/ZnO core/shell magnetic nanoparticles." *Materials Research Bulletin* 43.8-9 (2008): 2457-2468. https://doi.org/10.1016/j.materresbull.2007.07.035

[43]. M. Fu, Y. Li, S. wu, P. Lu, J. Liu, F. Dong, "Sol–gel preparation and enhanced photocatalytic performance of Cu-doped ZnO nanoparticles." *Applied Surface Science* 258.4 (2011): 1587-1591.https://doi.org/10.1016/j.apsusc.2011.10.003

[44]. J.H. Zheng, Q. Jiang, J.S. Lian, "Synthesis and optical properties of ZnO nanorods on indium tin oxide substrate." *Applied Surface Science* 258.1 (2011): 93-97. https://doi.org/10.1016/j.apsusc.2011.08.012

[45]. Zhang, D.F.; Zeng, F.B; "Characterization, activity and mechanisms of a visible light driven photocatalyst: Manganese and iron co-modified TiO_2 nanoparticles." *Russian Journal of Physical Chemistry A* 85.10 (2011): 1825. DOI: 10.1134/S0036024411100347

[46]. Justicia, I.; Ordejón, P.; Canto,G.; Mozos, J.L.; Fraxedas, J.; Battiston, G.A.; Gerbasi, R.; Figueras, A; "Designed self-doped titanium oxide thin films for efficient visible-light photocatalysis." *Advanced Materials* 14.19 (2002): 1399-1402. DOI: 10.1002/1521-4095(20021002)14:19

[47]. Q. Xiao, J. Zhang, C. Xiao, X. Tan, "Photocatalytic decolorization of methylene blue over Zn1− xCoxO under visible light irradiation." *Materials Science and Engineering: B* 142.2-3 (2007): 121-125. https://doi.org/10.1016/j.mseb.2007.06.021

[48. R. Geoge kutty, M.K. Seery, S.C. Pillai, "A highly efficient Ag-ZnO photocatalyst: synthesis, properties, and mechanism." *The Journal of Physical Chemistry C* 112.35 (2008): 13563-13570.DOI: 10.1021/jp802729a

[49]. Q. Xiao, L. Quyang, "Photocatalytic photodegradation of xanthate over Zn1− xMnxO under visible light irradiation." *Journal of Alloys and Compounds* 479.1-2 (2009): L4-L7. https://doi.org/10.1016/j.jallcom.2008.12.085

[50]. J.B. Zhong, J.Z. Li, X.Y. He, J. Zeng, Y. Lu, W. Hu, K. Lin, "Improved photocatalytic performance of Pd-doped ZnO." *Current Applied Physics* 12.3 (2012): 998-1001. https://doi.org/10.1016/j.cap.2012.01.003

[51]. J.B. Zhong, J.Z. Li, Y. Lu, X.Y. He, J. Zeng, W. Hu, Y.C. Shen, "Fabrication of Bi3+-doped ZnO with enhanced photocatalytic performance." *Applied Surface Science* 258.11 (2012): 4929-4933. https://doi.org/10.1016/j.apsusc.2012.01.121

[52]. J.-C. Sin, S.-M. Lam, K.-T. Lee, A.R. Mohamed, "Preparation and photocatalytic properties of visible light-driven samarium-doped ZnO nanorods." *Ceramics International* 39.5 (2013): 5833-5843. https://doi.org/10.1016/j.ceramint.2013.01.004

[53]. M. Ahmad, E. Ahmed, Y. Zhang, N.R. Khalid, J. Xu, M. Ullah, Z. Hong, "Preparation of highly efficient Al-doped ZnO photocatalyst by combustion synthesis." *Current Applied Physics* 13.4 (2013): 697-704. https://doi.org/10.1016/j.cap.2012.11.008

[54]. M. Rezaei, A. Habibi-Yangjeh, "Simple and large-scale refluxing method for preparation of Ce-doped ZnO nanostructures as highly efficient photocatalyst." *Applied Surface Science* 265 (2013): 591-596. https://doi.org/10.1016/j.apsusc.2012.11.053

[55]. R. Wang, J. H. Xin, Y. Yang, H. Liu, L. Xu, and J. Hu, "The characteristics and photocatalytic activities of silver doped ZnO nanocrystallites." *Applied Surface Science* 227.1-4 (2004): 312-317. https://doi.org/10.1016/j.apsusc.2003.12.012

[56]. K. Rekha, M. Nirmala, M. G. Nair, and A. Anukaliani, "Structural, optical, photocatalytic and antibacterial activity of zinc oxide and manganese doped zinc oxide nanoparticles." *Physica B: Condensed Matter* 405.15 (2010): 3180-3185. https://doi.org/10.1016/j.physb.2010.04.042

[57]. R. Chauhan, A. Kumar, and R. P. Chaudhary, “Photocatalytic studies of silver doped ZnO nanoparticles synthesized by chemical precipitation method,” Journal of Sol-Gel Science and Technology, vol. 63, no. 3, pp. 546–553, 2012. DOI: https://doi.org/10.1007/s10971-012-2818-3